PHYSICAL REVIEW LETTERS

Selection of Nonequilibrium Overlimiting Currents: Universal Depletion Layer Formation Dynamics and Vortex Instability

Gilad Yossifon and Hsueh-Chia Chang*

Department of Chemical and Biomolecular Engineering, Center for Microfluidics and Medical Diagnostics, University of Notre Dame, Notre Dame, Indiana 46556, USA

The ion flux dynamics across a straight nanoslot is imaged to understand the nonequilibrium phenomenon of overlimiting current density across a nanoporous membrane. With a slow ac field, an ion-depletion front is generated intermittently from one end of the nanochannel, and a vortex instability first predicted by Rubinstein, Staude, and Kedem [Desalination **69**, 101 (1988).] is found to arrest the self-similar diffusive front growth. This electrokinetic instability evolves into a stationary interfacial vortex array that specifies the overlimiting current, independent of external stirring or convective flow.

A curious and important *I-V* characteristic of conducting ion-selective membranes, such as Nafion membranes in fuel cells, cell membranes with ion channels, and desalination membranes, is that, at sufficiently high voltages, their current density often exceeds the limiting current density predicted by the classical diffusion-limited current transport theory [1] [see Fig. 1(d)]. Below the critical voltage for this overlimiting current, the *I-V* curve assumes initially a linear Ohmic relationship. Furthermore, an electroneutral diffusion region with a linear ion concentration gradient appears near the membrane interfaces to enhance the flux via diffusion [Fig. 1(a)]. This diffusive-flux enhanced current density saturates when both ion concentrations vanish at the surface [1]. Latter theories by Rubinstein and Shtilman [2] suggest that, at high voltages, an extended polarized layer (or, equivalently, space charge layer—SCL) much thicker than the electric Debye layer (EDL) can appear between the EDL and the electroneutral diffusion layer [DL; see Fig. 1(c)] to sustain the overlimiting current density, which can be much higher than the limiting current density. The collection of these three different regions is termed the concentration polarization layer (CPL). Based on this finding, Dukhin [3] postulated the existence of electrokinetic phenomena of the second kind.

A simple model for an ion-selective membrane is a straight nanoslot, within which the EDLs of both substrates overlap and whose ends feed into large reservoirs. Manazanares *et al.* [4] have averaged the nanopore surface charge across the membrane to produce an effective one-dimensional model, wherein the membrane is assumed to contain fixed charged groups at a uniform concentration Σ. Using such a model and arbitrarily selected Σ and membrane thickness d, the distinct dc ion distributions and *I-V* characteristics in the Ohmic and overlimiting current regimes are numerically computed from the ion transport and Poisson equations and are shown on both sides of a one-dimensional nanoslot or membrane in Fig. 1. Note that the depletion layer (a combination of the DL and the SCL,

hence, approximates the CPL thickness) on the left controls the *I-V* characteristics and exhibits all of the signature ion distributions in the various regimes. The enrichment side on the right with an ionic concentration higher than the bulk is always electroneutral (outside the thin equilibrium EDL) without a polarized layer.

Both the limiting current density sustained by a depletion layer without the SCL and the overlimiting current density sustained by a depletion layer with the SCL are dependent on the thickness of the CPL. However, there is no clear understanding of what selects this depletion layer thickness in the overlimiting region. If vigorous stirring exists in the system, it is typically assumed that the DL is the convection-diffusion layer due to external flow. The
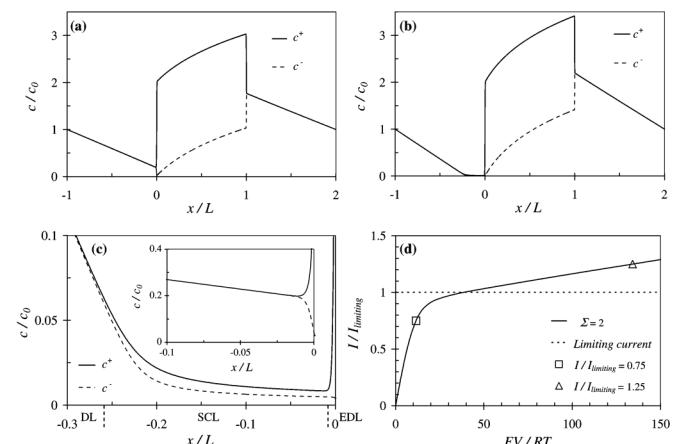
FIG. 1. Numerical computation results for the concentration polarization profiles across a membrane ($0 \leq x \leq 1$) for currents (a) below and (b) beyond the limiting current $I_{\lim}$. Part (c) depicts the ion concentration profiles on the anodic side of the membrane for the overlimiting conditions of (b), exhibiting an SCL, in contrast to the profile of (a) in the inset. The *I-V* curve for the membrane, exhibiting an inflection point at $I_{\lim}$, is shown in (d) with the conditions for (a) and (b) indicated. The value $\Sigma = 2$ (normalized by the bulk concentration c_0) and membrane thickness $d = 1$ (normalized by the CPL length) have been used.

limiting and overlimiting current density would then be dependent on the stirring rate. Electro-osmotic flows (EOFs) due to surface charge or an electro-osmotic (EO) vortex of the 2nd kind [3,5] on curved or inhomogeneous membranes can also produce stirring vortices to convectively control the ion flux at the membrane surface.

Another possible mechanism for selecting the depletion layer thickness involves an intrinsic instability of the SCL (see [6] and references therein), first reported by Rubinstein, Staude, and Kedem [7]. Unlike the Poisson-Boltzmann distribution, which is globally stable, the SCL with a constant flux is unstable to transverse perturbations in a manner reminiscent of Rayleigh-Benard and Marangoni instabilities in thermal conduction. Instead of a thermal gradient, the linear concentration gradient within the DL is perturbated by lateral osmotic pressure gradients that drive a vortex instability, provided the SCL exists within the CPL to produce the necessary space charge. The onset of the instability is controlled by an overvoltage [8], as is evident from the *I-V* curve in the inset in Fig. 4(b) wherein the overlimiting region, associated with this instability, appears only beyond a critical voltage (~ 20 V). This vortex instability develops into a stationary vortex array on the interface with a steady thickness. The critical thickness for the instability, which is independent of any bulk convection, then corresponds to the CPL thickness that controls the overlimiting current density. This mechanism is consistent with some indirect experimental observations: If the depletion layer is immobilized by a gel, overlimiting current is not observed, and the excess electric noise due to the vortices disappears [9]. However, direct experimental verification of this instability and how it selects the depletion layer thickness, which in turn determines the overlimiting current, has not been reported.

In recent years, fabrication of nanochannels with overlapping double layers has become possible, and the ion transport [10], ion-enrichment and ion-depletion [11], and overlimiting current [12] phenomena have been examined with these pseudo-one-dimensional ion-selective membranes. Kim *et al.* [12] have indeed measured current density beyond the limiting current density and correlated it to the depletion layer thickness. They also observed strong vortical motion in the overlimiting region. However, it is obvious from their design and images that there is significant EOF in their nanochannels, and such flow can produce vortices near channel corners due to field penetration [13] and hence may not be related to the depletion layer instability. Moreover, the vortices observed do not arrest the depletion growth, and their size is not linearly correlated to the depletion layer as was predicted by the theory [6,8]. Finally, they did not observe an array of vortices [6,8].

In this Letter, we report the first direct experimental proof for Rubinstein's instability by using an applied ac electric field to form the depletion layer intermittently at alternating ends of a linear nanoslot. A one-dimension theory is adequate because the instability occurs within

the depletion layer, which is at least 10 times smaller than the radius of curvature of the entrance, the length of the slot, and the microreservoir dimension [inset in Fig. 2(c)]. The field does vary somewhat at different locations along the entrance and leads to the slightly varying vortex size in Fig. 2(a), but there is very little lateral communication within the depletion layer. Moreover, due to flow continuity, the depth-averaged flow rate in the microchannel, where the depletion layer resides, must be equal to that in the nanoslot with a minute cross section area. Consequently, the average velocity in the depletion layer is extremely small, and EO convective contribution to the instability is negligible. As the DL is much thicker than the SCL, the formation dynamics of the depletion layer is dominated by the former. Quite fortuitously, the DL grows in a universal manner that allows us to precisely determine when vortices arrest this universal front evolution and select the CPL thickness. For symmetric electrolytes with negligible ion accumulation at the thin SCL, the DL is a diffusive front (that propagates into the Ohmic bulk solution) with a nearly constant flux S (positive when directed into the membrane surface), and the classical solution in a semi-infinite domain is [14] $C(x, t) = C_\infty - S/(2\sqrt{D})(2\sqrt{t/\pi}e^{-x^2/(4Dt)} - x/\sqrt{D}\{1 - \text{erf}[x/(2\sqrt{Dt})]\})$, where in the limit of large $x^2/(Dt)$, it simplifies to $C(x, t) \sim C_\infty - 2St^{3/2}\sqrt{D}e^{-x^2/(4Dt)}/x^2$. While the diffusive front has a concentration jump that is dependent on the flux S, the location of its front grows as $\sqrt{Dt}$ independent of S. Provided the flux is varied slowly, this self-similar front evolution dynamics stipulates that
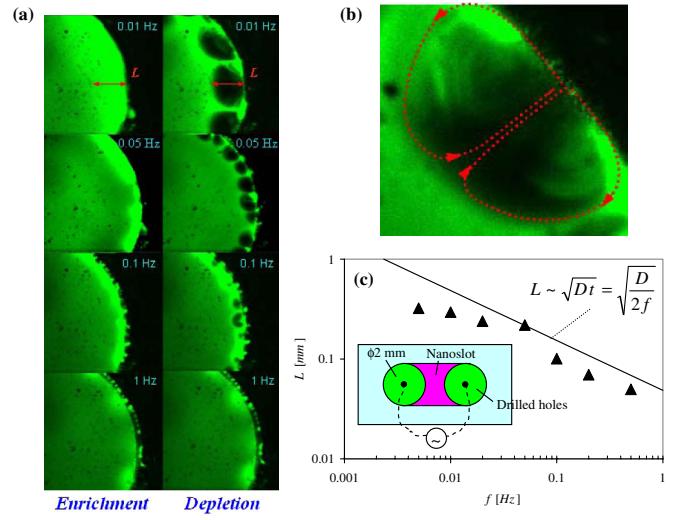
FIG. 2 (color online). (a) Confocal image snapshots of the maximum CPL extent L in its either enrichment (cathodic polarity) or depletion (anodic polarity) phase at different ac frequencies at the same voltage difference of 80 $V_{\text{p-p}}$ (peak to peak). (b) A close-up of one of the depletion regions showing its inner structure consisting of a vortex pair. (c) A Log-Log graph of the experimentally measured L (triangles) versus the frequency and also of a $\sqrt{Dt}$ trend line (continuous line). The inset shows the schematic configuration of the nanoslot device.

the thickness of the diffusive front is well described by the simple and universal diffusive scaling $\sqrt{Dt}$, independent of the frequency and the instantaneous electric field.

We exploit this field-independent universality of the depletion layer dynamics by using an ac (square-wave) field to sustain depletion layers of different thickness dynamically. Arrest of the growth of this DL by the instability would then be represented by a break from this universal dynamics. By using a low frequency (< 10 Hz), we should then be able to produce a depletion layer thickness $\sqrt{Dt}$ larger than 10 μm. Such a large thickness allows us to carry out fluorescent imaging of the depletion layer and to verify the vortex instability. As earlier instability theories [6–8] predict a particular scaling of the vortex pair wavelength to the depletion layer thickness, our images would allow us to verify the occurrence of the instability. There is no external stirring in our microdevice, and this mechanism for selecting the diffusion layer thickness is ruled out immediately. As our junction is nearly planar and perpendicular to the applied electric field, we do not expect an EO vortex of the second kind to develop. Any significant EO flow would disrupt the diffusive scaling.

The chip containing the micro/nanochannel junction was fabricated using standard photolithography technologies and consists of two large holes connected by a single nanoslot of 200 nm in depth and about 1 mm in length, d, at its center [inset in Fig. 2(c)]. Reservoirs were used on top of the holes wherein platinum electrodes (0.3 mm in diameter) were introduced. The two holes were drilled through a 1 mm thick Pyrex (Corning 7740) glass slide. The nanoslot was patterned on the other slide and etched through the α-Si layer. These two glass slides were then anodically bonded [15]. In order to visualize the polarized regions, we used either rhodamine dye molecules or fluorescently tagged human serum proteins in combination with confocal microscopy. All of the data and imaging are collected for phosphate buffered saline buffer and fluorescent molecules concentrations of 30 and 10 μM, respectively. This corresponds to a Debye length of about 55 nm, which assures a strong EDL overlap inside the nanoslot resulting in its cation permselectivity.

Figure 2(a) depicts the maximum extent of the enrichment and depletion layers at different frequencies in the range 0.01–1 Hz (see video in [16]). For frequencies higher than 1 Hz, the extent of the CPL is almost not discernible. As expected, due to its diffusive formation nature, the extent of the CPL is insensitive to whether it is in the enrichment or depletion phase. The most peculiar observation in Fig. 2(a) is the pattern formation in the depletion layer, while no such pattern exists in the enrichment phase. This is in agreement with the theory since an unstable SCL does not exist in the enrichment layer; hence, no instability can occur. Figure 2(b) is a blowup of one such depletion region revealing its inner structure, which consists of a vortex pair with streaks that resemble the streamlines from the simulation of Rubinstein and Zaltzman [8]. It is also

clear from the images that the vortex size decrease with the increase of the frequency (corresponds to the decrease of the CPL extent) while their number increase accordingly. Figure 2(c) depicts the maximum attainable depletion length versus different field frequencies. Also depicted is the simple $\sqrt{Dt}$ scaling of the CPL extent, wherein a reasonable value of $D \approx 4.7 \times 10^{-5}$ cm^2/s was chosen for the diffusion coefficient. Although vortices are observed within the evolving diffusion layer during this self-similar interval, they appear not to affect the diffusion layer growth. On the other hand, a clear break of this self-similar growth is observed beyond $t = 10$ s (0.01 Hz), corresponding to a critical diffusion layer thickness of 220 μm, and is associated with the fully established vortices that are responsible for the growth arrest. The arrest of the depletion layer also results in the arrest of the enrichment layer [cf. Fig. 2(a)]. The arrested CPL is still thin compared to the slot width, and hence boundary conditions should not contribute to the arrest of its growth.

Figure 3 depicts the instantaneous depletion layer (CPL) thickness for different frequencies. The higher-frequency values and the presaturation values for the low-frequency experiments collapse and obey the simple $\sqrt{Dt}$ scaling, suggesting that the universal diffusive formation dynamics is observed. That the self-similar diffusive scaling captures the front evolution dynamics supports the fact that convection is suppressed in our nanoslot device. A slight upward drift in the depletion layer thickness persists after the departure from the self-similar growth but at a much smaller rate than the diffusion scaling, before falling when the polarity changes. The slow drift is most likely because of small tangential ion migration due to the slight transverse curvature of the vortex array.

Figure 3 indicates that the CPL thickness is selected by the instability. The cross-plot of the imaged diffusion layer thickness against the vortex pair wavelength in Fig. 4(a)
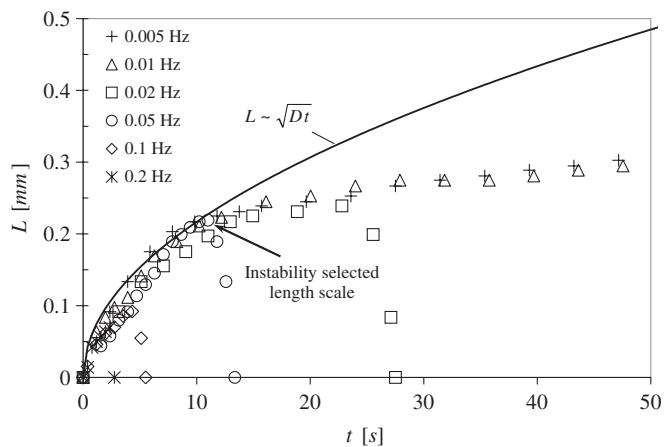
FIG. 3. Time evolution of the instantaneous depletion layer thickness for different frequencies at the same voltage difference of 80 $V_{\text{p-p}}$. Also depicted is the $\sqrt{Dt}$ scaling in a continuous line. A clear break from the self-similar scaling is observed at $L \sim$ 220 μm.

clearly shows that it obeys the linear scaling predicted by Zaltzman and Rubinstein [6,8] with an empirical coefficient of 1.25, another confirmation that it is the same instability (the complex process of wave length selection by small vortices breaks up through fusion and transformation into still larger vortices until a quasisteadylike pattern is formed can be seen in Fig. I of Ref. [16], which is in qualitative agreement with Figs. 5–11 of [8]).

Although the self-similar $\sqrt{Dt}$ dynamics is independent of voltage and frequency, the selected depletion layer thickness, represented by its value when it deviates from the self-similar $\sqrt{Dt}$ scaling (as indicated in Fig. 3), is independent of frequency but dependent on voltage, as shown in Fig. 4(b). The voltage dependence is inconsistent with Dukhin's prediction that the depletion layer thickness

should decrease as $1/E$ with respect to the field E, as it is assumed to be the convection-diffusion boundary layer generated by external stirring due to induced EO flow of the 2nd kind and hence scales as the $-1/2$ power of the flow, which is quadratic in E. This contradiction again suggests that the observed vortices are not due to natural EO flow or EO flow induced by the SCL but rather by the instability of the SCL. The saturation at high voltages most likely occurred because the CPL is now comparable in dimension to the nanoslot width, such that the curved front is no longer pseudo-one-dimensional. The measured I-V curve of the nanoslot shown in the inset in Fig. 4(b) indeed exhibits an overlimiting current regime beyond 20 V, in agreement with the observed onset voltage for the instability in the same figure, when it selects a CPL thickness.

We are grateful to Professor Y. Zhu, Professor A. Seabaugh, and Dr. S. Maheshwari for the use of their equipment and for their advice.
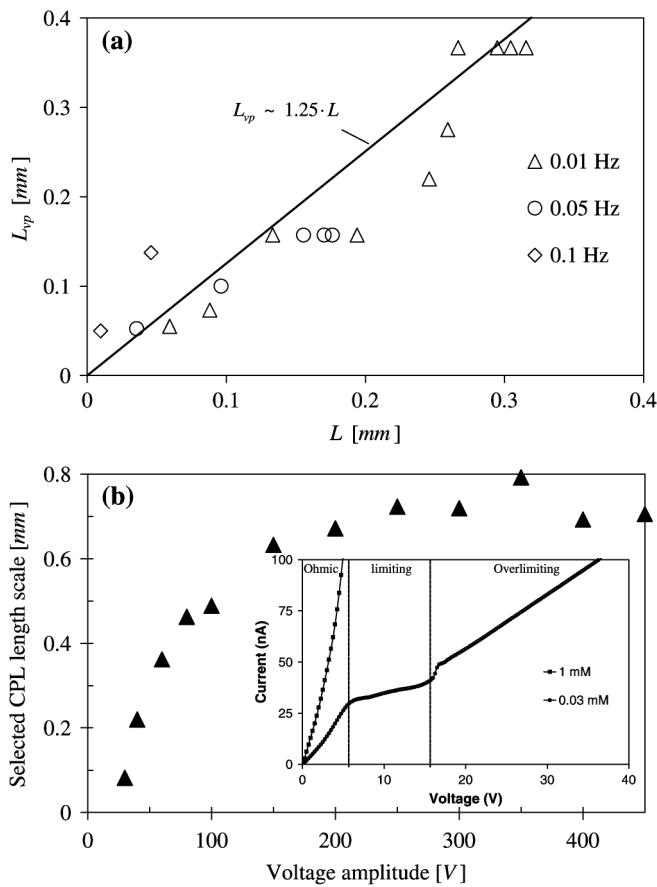
FIG. 4.   (a) Width of the periodicity cell L_{vp} versus the depletion layer length for different frequencies. (b) The instability selected CPL length scale as a function of voltage. The inset depicts the current sweep (0.25 V increments every 3 s, using Agilent Technologies 4155B semiconductor parameter analyzer) for two different ionic strengths, with the lower one corresponding to overlapping EDLs in the nanoslot showing three distinct I-V regimes with an overlimiting region beyond the same voltage (~ 20 V) as the onset of the instability.

*Corresponding author.
hchang@nd.edu

[1] V. G. Levich, *Physicochemical Hydrodynamics* (Prentice-Hall, New York, 1962).

[2] I. Rubinstein and L. Shtilman, J. Chem. Soc., Faraday Trans. 2 **75**, 231 (1979).

[3] S. S. Dukhin, Adv. Colloid Interface Sci. **35**, 173 (1991).

[4] J. A. Manazanares *et al.*, J. Phys. Chem. **97**, 8524 (1993).

[5] N. A. Mishchuk and P. V. Takhistov, Colloids Surf. A **95**, 119 (1995); Y. Ben and H.-C. Chang, J. Fluid Mech. **461**, 229 (2002).

[6] B. Zaltzman and I. Rubinstein, J. Fluid Mech. **579**, 173 (2007).

[7] I. Rubinstein, E. Staude, and O. Kedem, Desalination **69**, 101 (1988).

[8] I. Rubinstein and B. Zaltzman, Phys. Rev. E **62**, 2238 (2000).

[9] F. Maletzki, H. -W. Rosler, and E. Staude, J. Membr. Sci. **71**, 105 (1992); I. Rubinshtein *et al.*, Russ. J. Electrochem. **38**, 853 (2002).

[10] D. Stein, M. Kruithof, and C. Dekker, Phys. Rev. Lett. **93**, 035901 (2004).

[11] Q. Pu, J. Yun, H. Temkin, and S. Liu, Nano Lett. **4**, 1099 (2004).

[12] S. J. Kim *et al.*, Phys. Rev. Lett. **99**, 044501 (2007).

[13] S. K. Thamida and H. -C. Chang, Phys. Fluids **14**, 4315 (2002); G. Yossifon, I. Frankel, and T. Miloh, Phys. Fluids **18**, 117108 (2006).

[14] R. J. Hunter, *Foundations of Colloid Science* (Clarendon Press, Oxford, 1989), Vol. 2.

[15] V. G. Kutchoukov *et al.*, Sens. Actuators A, Phys. **114**, 521 (2004).

[16] See EPAPS Document No. E-PRLTAO-101-117852 for a supplementary video and figure. For more information on EPAPS, see http://www.aip.org/pubservs/epaps.html.